HHS Public Access

Author manuscript

Strahlenther Onkol. Author manuscript; available in PMC 2021 October 01.

Published in final edited form as:

Strahlenther Onkol. 2020 October ; 196(10): 900–912. doi:10.1007/s00066-020-01679-9.

The Role of Radiomics in Prostate Cancer Radiotherapy

Rodrigo Delgadillo, **John C. Ford**, **Matthew C. Abramowitz**, **Alan Dal Pra**, **Alan Pollack**, **Radka Stoyanova***

Department of Radiation Oncology, University of Miami Miller School of Medicine, Miami, FL 33136, USA

Abstract

"Radiomics", as it refers to the extraction and analysis of large number of advanced quantitative radiological features from medical images using high throughput methods, is perfectly suited as an engine of effectively sifting through the multiple series of prostate images from before, during, and following radiotherapy (RT). Multiparametric (mp) MRI, planning CT and cone beam CT (CBCT), routinely acquired throughout the RT and radiomics pipeline, are developed for extraction of thousands of variables. Radiomics data are in a format that is amicable for building descriptive and predictive models relating image features to diagnostic, prognostic or predictive information. The prediction of Gleason Score, the histop cancer grade, has been the mainstay of the radiomic efforts in prostate cancer. While Gleason Score (GS) is still the best predictor for treatment outcome, there are other novel applications of quantitative imaging that are tailored to RT. In this review, we summarize the radiomics efforts and discuss several promising concepts such as delta-radiomics and radiogenomics for utilizing image features for assessment of the aggressiveness of prostate cancer and its outcome. We also discuss opportunities for quantitative imaging with the advance of the instrumentation of MRI-guided therapies.

Keywords

Prostate Cancer; Radiomics; Multiparametric MRI; Cone Beam CT; Radiotherapy

1. INTRODUCTION

Contemporary radiation treatment (RT) of prostate cancer is associated with large-scale image acquisition. Multi-parametric magnetic resonance imaging (mpMRI), computed tomography (CT), cone beam CT (CBCT) are acquired at multiple steps of the course of RT, starting from patient diagnosis, treatment planning, delivery and follow-up. The sheer amount of data requires automated ways for extraction of quantitative imaging features and analysis for informing clinical decisions. Radiomics, as it refers to the extraction and

***Corresponding author:** Radka Stoyanova, Ph.D., Department of Radiation Oncology, University of Miami Miller School of Medicine, 1121 NW 14th St, Miami, Florida 33136, USA, Phone: (305)-243-5856, RStoyanova@med.miami.edu.

1.CONFLICT OF INTEREST

On behalf of all authors, the corresponding author states that there is no conflict of interest.

2.ETHICS APPROVAL

All patients have been enrolled in various institutional review board (IRB)-approved protocols for treatment of prostate cancer.

analysis of advanced quantitative information, converts imaging data into a high dimensional mineable feature space using a large number of automatically extracted data-characterization algorithms.[1] The main hypothesis behind the radiomics effort is that the imaging features capture distinct phenotypic differences of the tumors and may have diagnostic, prognostic, and predictive power.[2] Among the chief questions in the treatment of the prostate cancer are the choice of the RT fractionation schedule (hypo- or conventional fractionation) and the use, timing and duration of androgen deprivation therapy (ADT). Depending on the risk category, a considerable number of patients treated with RT present biochemical failure suggesting that additional strategies are needed for defining and treating patients based on improved risk stratification.

mpMRI has emerged as a major tool for prostate cancer detection and risk stratification.[3,4] An mpMRI exam is incorporated at all stages of the disease management, including screening, improving diagnostic accuracy, risk stratification, guiding treatment and post-treatment evaluation. The evaluation of the multiple sequences in the mpMRI is not trivial and there is large variability among radiologists in their detection of clinically significant prostate cancer.[5] To standardize the evaluation and reporting of mpMRI, the European Society of Urogenital Radiology (ESUR) published guidelines based on expert consensus in 2012, termed PI-RADS.[6] This reporting system utilizes a 1–5 score for each mpMRI sequence (T2-weighted (T2w) MRI, Dynamic Contrast Enhanced (DCE-MRI) and Diffusion Weighted Imaging (DWI)) and provides an overall score to each region of interest (ROI), with higher scores relating to a higher risk of aggressive cancer. For the relatively short time of its existence, the system has undergone several modifications (PI-RADS (v2)[7] and PI-RADS(v2.1)[8]) and admittedly, there is still significant inter-reader variability related to reader's experience.[9] PI-RADS was not designed for 3D tumor volume delineation and with respect to RT, PI-RADS has limited application in defining volumes (Gross Tumor Volume (s) (GTV(s)) for radiotherapy boost. Furthermore, the system is not defined for "irradiated" prostate and there is lack of quantitative assessment of imaging post-RT. Finally, the five-score system does not tap into the wealth of quantitative imaging information contained in the multiple sequences of mpMRI, nor does it elucidate inter- and intra-lesional spatial heterogeneity of prostate cancer. In contrast, the radiomics approach extracts large amounts of advanced quantitative mpMRI features in a format that is amicable for building descriptive and predictive models relating image features to gene-protein signatures or radiotherapy outcomes.[10]

The most widely used imaging modality in radiation oncology is CT, which assesses tissue density. In RT, the CT Hounsfield units are calibrated to electron density that allow for precise dose calculation. Consequently, CT images are of key use in RT planning. The radiomics features from CT also can have diagnostic and predictive power.[11,12] CBCT images are commonly used to check patient alignment prior to receiving treatment dose and important quantitative imaging information can be extracted from them.[13–15]

In this review, we discuss the impact of the radiomics efforts in RT of prostate cancer. First, the two main imaging modalities for prostate imaging, mpMRI and CT, are described. Then, the individual elements of the radiomics pipeline as tailored for RT are reviewed. The developments in prostate cancer radiomics for assessment of the aggressiveness of prostate

cancer are summarized. Finally, we review promising applications of radiogenomics, delta-radiomics, and the opportunities for serial image analysis from MRI-guided radiotherapy (MRIgRT) for prognostic assessment and treatment management.

2 IMAGING MODALITIES FOR PROSTATE CANCER RT

2.1 Multiparametric MRI of the prostate

With its superior soft tissue contrast over x-ray based imaging methods, mpMRI has become routinely used in the radiation oncology clinical workflow for pre-treatment planning and follow-up assessment.[16] Diagnostic MRI scanners can utilize functional MRI methods that are sensitive to tumor biology, which are increasingly employed for tumor detection and delineation.[17] mpMRI combines functional (perfusion via DCE-MRI and diffusion via DWI)[18–20] and anatomical information (T2w-MRI)[21] that enhances diagnostic reliability. An Apparent Diffusion Coefficient (ADC) map is calculated on the MRI scanner's console. In mpMRI, T2w provides clear delineation of prostatic zonal anatomy. DCE takes advantage of vascular differences between malignant lesions and surrounding prostatic tissue to facilitate target identification. ADC is associated with the density of diffusion barriers and exploits the higher cellular density and more complex intracellular microstructure in relative benign prostatic tissue to differentiate malignant lesions.

The correlation of radical prostatectomy histopathology with the mpMRI's sequences is illustrated in Figure 1. There is no other imaging modality that has demonstrated the same sensitivity and specificity for distinguishing intraprostatic cancer of higher grade (Gleason Score (GS) 7 or above).[22,23]

There is a burgeoning literature on the use of external beam radiotherapy to treat the dominant intraprostatic lesion (DIL) mpMRI directed RT,[24–26] including favorable preliminary toxicity results from the FLAME, a randomized clinical trial.[27] For effective treatment, the areas of most aggressive disease need consistent and objective identification in 3D. Prostate cancer exhibits spatio-temporal heterogeneity that can confound imaging interpretation and selection of boost volume. Over 70% of prostate cancers are multi-focal,[28] and neither large volume, nor multifocality are necessarily inherent features of aggressiveness.[29] Therefore, targeting dominant nodules can still miss the most aggressive disease, causing misinformed treatment decisions.[30]

Tumor heterogeneity can be elucidated by mapping sub-regions of the lesion with differential imaging characteristics, called habitats.[31–33] Delineating tumor habitats *in vivo* is important for determining prognosis and providing effective treatment. Simply detecting tumors may not be enough; the full degree of tissue heterogeneity must also be understood.

We proposed the prostate tumor habitat risk scoring (HRS) system that scores the voxels in the prostate by level of aggressiveness.[34] HRS is using referenced DCE sequences and ADC maps to generate a 10-point heat map for automatic delineation of GTVs. First, a quantitative DCE-MRI analysis, based on unsupervised pattern recognition[35] assigns to each pixel a score, related to aggressiveness.[36] The algorithm uses a normalization of the tumor's DCE signal to muscle (Gluteus Maximus).[35] Second, a quantitative ADC score is also

assigned to each pixel, based on identified optimal Apparent Diffusion Coefficient (ADC) thresholds for automatic delineation and risk assignment of prostatic lesions.[37] The quantitative DCE and ADC analyses were combined and optimized by referencing to prostatectomy GSs and lesion volumes. The HRS contours are implemented in the radiomics pipeline (Figure 2) and migrated to the planning CT for boost volume generation. The details for HRS construction and implementation an imaging analysis platform, MIM (MIM software, Cleveland, OH) are given in Stoyanova *et al*.[34]

2.2 CT of the prostate

CT images are widely used in RT for dose calculation using the CT Hounsfield units. MRI units are not directly related to electron density and although attempts have been made to generate dose calculations from MRI by generating synthetic CT images,[38–41] CT continues to be the standard modality for RT dose calculation. CT depicts in 3D the patient anatomy and CT-based radiomics models have been extensively used in lung, for example.[42] Recently, the modality is used to extract radiomic features in prostate cancer.

3. RADIOMICS PIPELINE OF PROSTATE CANCER RT

The steps in the radiomic pipeline for RT of prostate cancer are shown in Figure 2 and discussed in detail in our previous reviews.[32,43] The radiomic process starts with image acquisition as discussed above. For illustration, the input images from the same patient: mpMRI, CT, and CBCT are displayed. For mpMRI, the T2w, DWI at high b-value (1000 s/mm^2), ADC and the early enhancing image in the DCE-MRI are shown.

The segmentation of volumes of interest (VOI) is a key process because it specifies the region which radiomic data will be extracted. In the prostate, the transition zone (TZ) and peripheral zone (PZ) are segmented, because the zones have different imaging characteristics in mpMRI and are often analyzed separately (Figure 2, second panel). Automated or partially automated delineations for the prostate and its zone are being explored in current research.[44,45] Further, the heat map of the HRS, depicting the pixels with HRS ≥ 6 is displayed. The area of the tumor is clearly depicted and further delignated by the contour of HRS6. The volume, defined by pixels with HRS = 6 was in good agreement with radical prostatectomy lesion volumes[34] and we chose HRS = 6 to serve both as VOI for extraction of radiomics variables as well as for automatic segmentation of volumes for GTV for RT dose boost. Finally, the regions of normal appearing PZ and TZ (NAPZ, NATZ) are automatically determined by subtracting the HRS6 contour from PZ and TZ.

Radiomics feature extraction, which follows volumes segmentation, are discussed in detail in our previous work.[43] In general, they can be categorized into: ***(i)*** morphological, ***(ii***) semantic, ***(iii)*** statistical, and ***(iv)*** transform-based radiomic features. Briefly, morphological features describe the form and structure of the VOI, which can range from geometrical descriptions that are simple, such as volume, to metrics that are complicated, such as fractal dimensions.[46–48] Semantic features are quantitative descriptors derived empirically by the radiologist when assessing mpMRI for improved detection, location, and risk stratification in patients with prostate cancer, such as those defined in PI-RADS.[7] First order statistical features are related to the intensity histogram of the VOI, whereas higher order statistical

features are first encoded into different matrix types describing how collections of grey levels within the VOI relate to one another.[49–52] Transform-based features are features extracted following a kernel transformation of the VOI, which includes but is not limited to the Fourier transform, Gabor transform, wavelet transform, Laplacian transforms of Gaussian bandpass filters.[53–55] Of a note, HRS as a construct of ADC intensities and DCE-curves can be considered a lower dimensional radiomics score.

Data integration and application in RT are the remaining steps in the radiomics pipeline, (Figure 2, fourth and fifth panel, respectively). Examples will be further explored in the remaining sections of the paper. Data integration refers to the practice of combining radiomics data with other available biomarkers. The hope is that assimilation of more biomarkers will result in models that are more complete. Many applications in RT of prostate may be possible including aiding and improving diagnostic establishment, patient-individualized treatment, predictive accuracy, and prognostic accuracy.

4. OVERVIEW OF RADIOMICS EFFORTS FOR PROSTATE CANCER

The radiomics publications in prostate cancer are summarized in Table 1; this summary is updated from our 2016 and 2018 radiomics reviews.[32,43] The publications are further presented in Figure 3 per year and per imaging modality from which the radiomic features were extracted. There is a sharp increase in the publications per year from 2017 to 2019. At the time of writing of this review, we are only partially through the year and the number of publications is already nearly equal to the previous year.

A variety of radiomics features are considered in assessing the prostate cancer aggressiveness. Figure 4 demonstrates that proportion of these publications according to the five categories of radiomics features discussed earlier. Often studies are not limited to a single category of radiomics features. Statistical features were used alone in 45% of these publications with 91% of them considering statistical radiomics features in some form. Consequently, statistical radiomics features are by far the most commonly used category.

The majority (86%) of the radiomics approaches used GS as an analysis endpoint. Comparison between the GS studies is not straightforward because a variety of thresholds are considered as an end-point. In some studies, GS is used in combination with another analysis endpoint. Varghese *et al.*[56] and Osman *et al.*[11] used GS in combination with tumor grade and PSA for risk stratification. Cuocolo *et al.*[57] used GS in combination with max cancer core length an analysis endpoint. Algohary *et al.*[58] used PI-RADS score and biopsy positivity as analysis endpoints. Shiradkar *et al.*[59] and Bourbonne *et al.*[60] used biochemical recurrence (BCR) as analysis endpoints.

MRI-based radiomic features were used in model building of 91% of studies that assessed tumor aggressiveness. As shown in Figure 3b, the most used imaging modality (68% of publications) was biparametric (bi)MRI (acquisition protocol that uses only T2w and DWI). bpMRI is becoming an attractive alternative to mpMRI because it is faster and cost-effective.[61] In addition, the benefit of DCE-MRI for prostate cancer characterization is still a matter of debate (in the current PI-RADSv2.1[8] the DCE sequence is used in only determination).

Even though CT images are highly repeatable, only two CT-based radiomics studies of prostate cancer to date were found.[11,12] Because of the availability of CTs in RT, we discuss these efforts in more details. Osman *et al.* found that classifiers developed from CT-based radiomics were well performing in distinguishing GS < 7 vs GS ≥7 (AUC = 0.90), GS 3+4 vs 4+3 (AUC = 0.96), low vs high risk groups (0.96), and low vs intermediate risk group (AUC = 1.00) for their training set, but only modest performance with their validation data sets. The authors clarify that the modest performance of the validation data sets may be due to small number of patients and class imbalances in the validation data sets.[11] Another study by Tanadini-Lang *et al.*[12] evaluated radiomics features of CT perfusion and found classifiers that distinguished well between GS=7 and GS>7 (AUC = 0.81) and moderately between GS = 3+4 and GS = 4+3 (AUC = 0.77). No validation data set was included in Tanadini-Lang *et al.* These exploratory studies indicate possible areas of future research and prognostic potential using CT-based radiomics of prostate cancer.

The performance of the models is summarized in the last column of Table 1. The direct comparison between the different approaches is difficult because ***(i)*** the variety of the used models' endpoints (Gleason Score (either from biopsy or prostatectomy), PSA, PIRADS, biochemical recurrence (BCR), etc.); and ***(ii)*** the variety of reported performance evaluation metrics - AUC, specificity, accuracy, etc.

5. THE PROMISE OF RADIOMICS FOR TREATMENT RESPONSE

Below we summarize novel concepts and efforts in the field with the emphasis of their utilization in RT of prostate cancer.

5.1. Delta-radiomics

Delta-radiomics refers to changes in radiomics features over time. Radiomics feature trends seen in longitudinal imaging studies over the course of therapy may add important clinical information such as treatment response prediction.[62] A recently published work[63] found that MRI-based delta-radiomics models of 33 prostate cancer patients had lower predictive performance than models using pre- or post-treatment MR images; however, that study utilized only two time points.

A recent analysis of 23 patients enrolled in the Phase I Trial of MRI-Guided Prostate Cancer Lattice Extreme Ablative Dose (LEAD) Boost Radiation Therapy at University of Miami[64] exploits one pre-treatment and three post-treatment MRIs to study radiation-induced changes in quantitative radiomics features. A schematic of the MR imaging workflow is shown in Figure 5. Prior to the treatment planning CT simulation, radio-opaque fiducial markers are placed in the prostate to enable on-board CBCT-based set up for subsequent radiation treatment. A Planning MRI, acquired at the same time as the CT simulation, facilitates fusion #3 of the Diagnostic mpMRI to the Planning CT via fusion #1 of the Diagnostic and Planning MRIs and fiducial-based fusion #2 of the Planning MRI and CT. The post-treatment MRIs at 3 and 9 months and the final pre-biopsy MRI at 2–2.5 years are fused (#4–6) to the pre-treatment MRIs. Radiomic features are thus readily extracted from regions of interest on MRIs over multiple timepoints before and after radiotherapy. Shown in Figure 6 are the extracted values of ADC and v_e (relative volume of the extravascular

extracellular space) for the GTV, NATZ and NAPZ, pre- and post-RT. The increases in ADC and v_e with RT are expected: viable tumor is characterized by an increased 'cellularity', or relatively large intracellular space. Since intracellular water diffusion is more restricted inside the cell than in the interstitial space, a loss in cellularity results in an increase in ADC, and of course the increase in interstitial space results in increased v_e. It is interesting that there is a substantial and persistent increase in v_e in the NATZ following RT. The pathophysiologic mechanism underlying this and other apparent trends in the data will be the subject of future work.

5.2. Cone Beam CT

Radiomics features from CBCT images may provide an opportunity to efficiently capture early tumor response to therapy and allow for adaptive treatment decisions though there are image quality challenges. To date, most radiomics studies of prostate cancer are limited to assessments before treatment or with limited time points. CBCT scans are typically captured daily for patient alignment prior to RT as part of standard care. Consequently, CBCT images offer the advantage of adding radiomics data during the course of treatment at multiple time points. However, CBCT image quality in comparison to diagnostic CT has known limitations in the form of more beam hardening, motion, scatter, and other artifacts.[65–68] The viability of radiomics analysis of CBCT image rests largely on whether CBCT image is sufficient to capture repeatable and reproducible radiomic features. Although not focused on prostate cancer, there are some published studies focused on radiomic feature quality of CBCT images.[13,69,70] In a pilot study, we studied the repeatability of CBCT-based radiomic features of 20 CBCT test-retest image pairs and the reproducibility of radiomic features between the planning CT and the first fraction CBCT for 20 patients. We determined that the CBCT reconstruction and image preprocessing methods affect the repeatability and reproducibility of radiomic features. In view of the viability of CBCT-based radiomics it remains to be seen whether the radiomics features will also have prognostic power. For other cancer sites, like non-small cell lung cancer, well-performing prognostics models using CBCT-based radiomics have been documented.[14,15] Considering the previous studies of CBCT radiomic quality and the potential shown in cancer sites, CBCT radiomics may yet be viable for the prediction of treatment outcome.

5.3. MRI-guided Radiotherapy

The integration of the MRI scanner with the linear accelerator radiation delivery machine has launched a new era for radiotherapy.[71] On-board MRI-guided radiotherapy (MRIgRT) not only provides for increased setup accuracy but also affords improved motion management as well as the capability for on-table adaptive re-planning based on the anatomy of the day. Precise localization of the tumor and nearby organs at risk in real time has allowed for safe tumor dose escalation on hybrid MRI/RT machines.[72] In addition, on-board MRIgRT holds promise for improving prognostic assessment of cancer patients via MRI set-up images that are acquired daily on these machines. Prior to the advent of hybrid MRI/RT treatment platforms, MR images were typically acquired only pre- and post-treatment clinically, and perhaps once or twice during treatment in the clinical research setting. Daily MR images from MRIgRT now provide a wealth of image data during the entire course of treatment with vastly improved temporal resolution, offering a potentially

valuable new assessment tool via delta-radiomics. Recent studies conducted on low-field (0.35T) hybrid MRI/RT machines have shown the promise of MRI-derived radiomic biomarkers to predict response in rectal cancer[73] and pancreatic cancer.[74] Future studies will determine whether radiomics analysis of daily images from MRIgRT can similarly add prognostic value to prostate cancer treatment.

5.4. Radiogenomics

Tumor underlying molecular and genomic characteristics can provide patient-tailored treatment stratification and prediction of therapy response that goes beyond the Gleason Score's prediction of aggressiveness. There is an increasing interest in the assessment of the association of radiomics features with biopsy tissue genomics. In the first radiogenomics study, we demonstrated significant correlation of mpMRI radiomics with prostate cancer risk gene expression profiles in mpMRI-guided biopsies tissues.[75] Imaging features clustered with gene markers are associated with adverse outcome. Another group using a proliferation gene signature found similar results,[76] supporting a role for the radiomics features associated with gene expression patterns in quantitative imaging algorithms.

The presence of hypoxia in the tumor microenvironment, associated with a more aggressive tumor phenotype,[77,78] often underlies the resistance to RT in comparison with well-vascularized, well-oxygenated tumors.[77,79–81] Thus, *in vivo* knowledge of the spatial distribution of hypoxia in tumors may provide prognostic information and can possibly improve treatment planning (e.g. intensity-modulated radiotherapy).[81] Dynamic Contrast Enhanced (DCE-) MRI can characterize the microenvironment in solid tumors by determining areas of inadequate or heterogeneous perfusion with hyper-permeable vasculature which are related to the degree of hypoxia.[82] The individual tumor habitats vary in their rate and magnitude of contrast uptake and washout.[83] In a pilot study, we analyzed twenty genes in 17 biopsy cores from six patients (Figure 7). The hierarchical clustering on expression from these genes identified reciprocal heat-map patterns in the cores from two high-risk patients in the dataset. Analysis of the DCE-MRI curves confirmed that the patients had dramatically different contrast uptake patterns, suggesting the potential of DCE radiomics to predict for hypoxia.

Gene expression signatures, such as Decipher® (DecipherDx, San Diego, California),[84–87] Prolaris® Cell Cycle Progression (CCP) (Myriad Genetics, Salt Lake City, Utah),[88–93] and Genomic Prostate Score® (GPS) (Genomic Health, Redwood City, CA)[93–96] add to clinical-pathologic risk factors and have the potential to become integral to risk stratification and management. Significant correlation between mpMRI radiomics with prostate cancer risk gene expression signatures was demonstrated in mpMRI-guided biopsies tissues.[75,97] Hectors *et al.*,[97] report numerous significant associations of mpMRI radiomics features with the gene signature PORTOS,[98] which has recently been reported as promising for prediction of outcome (i.e. development of distant metastasis) after postoperative radiation therapy of prostate cancer. The significant correlations between multiparametric MRI radiomics features and PORTOS suggest that mpMRI radiomics analysis may be useful for prediction of salvage radiotherapy outcome.

6. DISCUSSION

As a topic of interest in research, radiomics of prostate cancer has received increasing attention in recent years. The number of published studies have almost quadrupled in the two years since our previous review paper.[43] MRI is still the main modality for radiomics studies, but CT and CBCT-based features are progressively being investigated. These datasets, specifically acquired in the course of RT, as well as the emerging MRIgRT capabilities, provide RT clinicians and researchers with unique opportunities for investigations. Developing tools and pipelines for optimal extraction of radiomics features holds the promise for improved prognostic and predictive assessment for prostate cancer.[99]

RT of prostate cancer also poses specific questions that are not readily answered with the existing imaging and radiomics workflows. PI-RADS cannot provide the 3D volume of the radiation boost, nor they are defined in the setting of radiated prostate. The goal of a majority of radiomics studies is to predict GS, an information that is readily available for the radiation oncologist. In the summary of manuscripts in Table 1, only two publications (9%) predict for BCR. Intermediate and high-risk prostate cancer patients, who are candidates for RT, are very heterogeneous in terms of progression risk. While there is a gradation of treatment intensification options that are effective, optimized criteria are lacking for recommendations concerning RT dose, RT fractionation, the use, timing and duration of ADT and the use of additional systemic agents (e.g., abiraterone, chemotherapy).

These questions frame the role of imaging in the identification of early markers of patient outcome. Prostate cancer has an exceptionally long natural history and the lack of mature datasets with available outcome end-points poses a particular challenge for these studies.

One area of prosate cancer radiomics research that holds particular promise is delta-radiomics. With the advent of MRIgRT, we now have access to daily MRI patient set-up images for patients treated on MRIgRT machines in addition to daily CBCT images for patients treated on conventional linacs. There is tremendous potential in mining this wealth of imaging data to discover trends in radiomics features during treatment that could be exploited for predicting treatment response or normal tissue toxicity. Correlating these trends with patient outcome could lead to predicitve models that the radiation oncologist would utilize to guide possible changes in treatment early on, thus realizing the vision of personalized care tailored to the individual patient. However, this approach is not without challenges. Development of reliable predictive models using machine learning typically require on order of hundreds of patients to use as input for building the model, in addition to a like number of patients in an independent data set for model validation. Use of retrospective image data can be problematic, as it is well known that radiomic features can be sensitive to image acuisition parameters and reconstruction algorithms, which vary over institutions and even from patient to patient within a given clinic. Efforts are underway to determine which MRI- and CBCT-based radiomic features are repeatable (i.e., robust to test/retest on a given machine) and reproducible (i.e., constant across machine platforms). While repeatability and reproducibility of radiomic features are necessary and desirable, the ultimate test is the ability of radiomic features used in a model to reliably predict patient outcome.

In conclusion, this review paper has summarized ongoing radiomics efforts for analysis of imaging studies, acquired from prostate cancer imaging prior, during and after radiation treatment. The correlation to patient outcomes, rather than surrogate pathological features, is still challenging, but more groups are developing such models. It will be important to incorporate radiomics-based models into clinical trials to properly validate its robustness, maximize efficacy and confirm the clinical utility of these tools. The expectation is that these concepts, methods and tools described herein will be eventually applicable to the radiation oncology practice.

7. REFERENCES:

1. Gillies RJ, Kinahan PE, Hricak H. Radiomics: Images Are More than Pictures, They Are Data. Radiology. 2016;278(2):563–577. [PubMed: 26579733]
2. Aerts HJ, Velazquez ER, Leijenaar RT, et al. Decoding tumour phenotype by noninvasive imaging using a quantitative radiomics approach. Nat Commun. 2014;5:4006. [PubMed: 24892406]
3. Ahmed HU, El-Shater Bosaily A, Brown LC, et al. Diagnostic accuracy of multi-parametric MRI and TRUS biopsy in prostate cancer (PROMIS): a paired validating confirmatory study. Lancet. 2017;389(10071):815–822. [PubMed: 28110982]
4. Futterer JJ, Briganti A, De Visschere P, et al. Can Clinically Significant Prostate Cancer Be Detected with Multiparametric Magnetic Resonance Imaging? A Systematic Review of the Literature. Eur Urol. 2015;68(6):1045–1053. [PubMed: 25656808]
5. Israel B, Leest MV, Sedelaar M, Padhani AR, Zamecnik P, Barentsz JO. Multiparametric Magnetic Resonance Imaging for the Detection of Clinically Significant Prostate Cancer: What Urologists Need to Know. Part 2: Interpretation. Eur Urol. 2020;77(4):469–480. [PubMed: 31767492]
6. Barentsz JO, Richenberg J, Clements R, et al. ESUR prostate MR guidelines 2012. Eur Radiol 2012;22(4):746–757. [PubMed: 22322308]
7. Weinreb JC, Barentsz JO, Choyke PL, et al. PI-RADS Prostate Imaging - Reporting and Data System: 2015, Version 2. Eur Urol. 2016;69(1):16–40. [PubMed: 26427566]
8. Turkbey B, Rosenkrantz AB, Haider MA, et al. Prostate Imaging Reporting and Data System Version 2.1: 2019 Update of Prostate Imaging Reporting and Data System Version 2. Eur Urol. 2019;76(3):340–351. [PubMed: 30898406]
9. Stabile A, Giganti F, Kasivisvanathan V, et al. Factors Influencing Variability in the Performance of Multiparametric Magnetic Resonance Imaging in Detecting Clinically Significant Prostate Cancer: A Systematic Literature Review. Eur Urol Oncol. 2020;3(2):145–167. [PubMed: 32192942]
10. Kumar V, Gu Y, Basu S, et al. Radiomics: the process and the challenges. Magn Reson Imaging. 2012;30(9):1234–1248. [PubMed: 22898692]
11. Osman SOS, Leijenaar RTH, Cole AJ, et al. Computed Tomography-based Radiomics for Risk Stratification in Prostate Cancer. International Journal of Radiation Oncology*Biology*Physics. 2019;105(2):448–456.
12. Tanadini-Lang S, Bogowicz M, Veit-Haibach P, et al. Exploratory radiomics in computed tomography perfusion of prostate cancer. Anticancer research. 2018;38(2):685–690. [PubMed: 29374691]
13. Fave X, Zhang L, Yang J, et al. Impact of image preprocessing on the volume dependence and prognostic potential of radiomics features in non-small cell lung cancer. Transl Cancer Res. 2016;5(4):349–363.
14. van Timmeren JE, Leijenaar RTH, van Elmpt W, et al. Survival prediction of non-small cell lung cancer patients using radiomics analyses of cone-beam CT images. Radiotherapy and Oncology. 2017;123(3):363–369. [PubMed: 28506693]
15. Qin Q, Shi A, Zhang R, et al. Cone-beam CT radiomics features might improve the prediction of lung toxicity after SBRT in stage I NSCLC patients. Thoracic Cancer. 2020;n/a(n/a).

16. Jones KM, Michel KA, Bankson JA, Fuller CD, Klopp AH, Venkatesan AM. Emerging Magnetic Resonance Imaging Technologies for Radiation Therapy Planning and Response Assessment. Int J Radiat Oncol. 2018;101(5):1046–1056.
17. Chandarana H, Wang H, Tijssen RHN, Das IJ. Emerging role of MRI in radiation therapy. J. Magn. Reson. Imaging 2018;48(6):1468–1478. [PubMed: 30194794]
18. Vargas HA, Akin O, Franiel T, et al. Diffusion-weighted endorectal MR imaging at 3 T for prostate cancer: tumor detection and assessment of aggressiveness. Radiology. 2011;259(3):775–784. [PubMed: 21436085]
19. Somford DM, Hoeks CM, Hulsbergen-van de Kaa CA, et al. Evaluation of diffusion-weighted MR imaging at inclusion in an active surveillance protocol for low-risk prostate cancer. Investigative radiology. 2013;48(3):152–157. [PubMed: 23328910]
20. Peng Y, Jiang Y, Yang C, et al. Quantitative analysis of multiparametric prostate MR images: differentiation between prostate cancer and normal tissue and correlation with Gleason score--a computer-aided diagnosis development study. Radiology. 2013;267(3):787–796. [PubMed: 23392430]
21. Hegde JV, Mulkern RV, Panych LP, et al. Multiparametric MRI of prostate cancer: an update on state-of-the-art techniques and their performance in detecting and localizing prostate cancer. J Magn Reson Imaging. 2013;37(5):1035–1054. [PubMed: 23606141]
22. Isebaert S, Van den Bergh L, Haustermans K, et al. Multiparametric MRI for prostate cancer localization in correlation to whole-mount histopathology. J Magn Reson Imaging. 2013;37(6):1392–1401. [PubMed: 23172614]
23. Futterer JJ, Briganti A, De Visschere P, et al. Can Clinically Significant Prostate Cancer Be Detected with Multiparametric Magnetic Resonance Imaging? A Systematic Review of the Literature. Eur Urol 2015.
24. Timon G, Ciardo D, Bazani A, et al. Short-term high precision radiotherapy for early prostate cancer with concomitant boost to the dominant lesion: ad interim analysis and preliminary results of Phase II trial AIRC-IG-13218. Br J Radiol. 2018:20160725. [PubMed: 29750539]
25. von Eyben FE, Kiljunen T, Kangasmaki A, Kairemo K, von Eyben R, Joensuu T. Radiotherapy Boost for the Dominant Intraprostatic Cancer Lesion-A Systematic Review and Meta-Analysis. Clin Genitourin Cancer. 2016;14(3):189–197. [PubMed: 26768965]
26. Bauman G, Haider M, Van der Heide UA, Menard C. Boosting imaging defined dominant prostatic tumors: a systematic review. Radiother Oncol. 2013;107(3):274–281. [PubMed: 23791306]
27. Monninkhof EM, van Loon JWL, van Vulpen M, et al. Standard whole prostate gland radiotherapy with and without lesion boost in prostate cancer: Toxicity in the FLAME randomized controlled trial. Radiother Oncol. 2018;127(1):74–80. [PubMed: 29336835]
28. Wolters T, Montironi R, Mazzucchelli R, et al. Comparison of incidentally detected prostate cancer with screen-detected prostate cancer treated by prostatectomy. Prostate. 2012;72(1):108–115. [PubMed: 21538424]
29. Wolters T, Roobol MJ, van Leeuwen PJ, et al. Should pathologists routinely report prostate tumour volume? The prognostic value of tumour volume in prostate cancer. European urology. 2010;57(5):821–829. [PubMed: 19664875]
30. Klotz L Active surveillance for prostate cancer: overview and update. Current treatment options in oncology. 2013;14(1):97–108. [PubMed: 23318986]
31. Gatenby RA, Grove O, Gillies RJ. Quantitative imaging in cancer evolution and ecology. Radiology. 2013;269(1):8–15. [PubMed: 24062559]
32. Stoyanova R, Takhar M, Tschudi Y, et al. Prostate cancer radiomics and the promise of radiogenomics. Transl Cancer Res. 2016;5(4):432–447. [PubMed: 29188191]
33. Stoyanova R, Pollack A, Takhar M, et al. Association of multiparametric MRI quantitative imaging features with prostate cancer gene expression in MRI-targeted prostate biopsies. Oncotarget. 2016.
34. Stoyanova R, Chinea F, Kwon D, et al. An Automated Multiparametric MRI Quantitative Imaging Prostate Habitat Risk Scoring System for Defining External Beam Radiation Therapy Boost Volumes. Int J Radiat Oncol Biol Phys. 2018.
35. Chang YC, Ackerstaff E, Tschudi Y, et al. Delineation of Tumor Habitats based on Dynamic Contrast Enhanced MRI. Sci Rep. 2017;7(1):9746. [PubMed: 28851989]

36. Parra NA, Pollack A, Chinea FM, et al. Automatic Detection and Quantitative DCE-MRI Scoring of Prostate Cancer Aggressiveness. Front Oncol. 2017;7:259. [PubMed: 29177134]
37. Tschudi Y, Pollack A, Punnen S, et al. Automatic Detection of Prostate Tumor Habitats using Diffusion MR. Scientific Reports. 2018.
38. Jonsson JH, Karlsson MG, Karlsson M, Nyholm T. Treatment planning using MRI data: an analysis of the dose calculation accuracy for different treatment regions. Radiation Oncology. 2010;5(1):62. [PubMed: 20591179]
39. Rasch C, Barillot I, Remeijer P, Touw A, van Herk M, Lebesque JV. Definition of the prostate in CT and MRI: a multi-observer study. International Journal of Radiation Oncology*Biology*Physics. 1999;43(1):57–66.
40. Siversson C, Nordström F, Nilsson T, et al. Technical Note: MRI only prostate radiotherapy planning using the statistical decomposition algorithm. Medical Physics. 2015;42(10):6090–6097. [PubMed: 26429284]
41. Liu Y, Lei Y, Wang Y, et al. Evaluation of a deep learning-based pelvic synthetic CT generation technique for MRI-based prostate proton treatment planning. Physics in Medicine & Biology. 2019;64(20):205022. [PubMed: 31487698]
42. Shafiq-Ul-Hassan M, Latifi K, Zhang G, Ullah G, Gillies R, Moros E. Voxel size and gray level normalization of CT radiomic features in lung cancer. Sci Rep. 2018;8(1):10545. [PubMed: 30002441]
43. Yang F, Ford JC, Dogan N, et al. Magnetic resonance imaging (MRI)-based radiomics for prostate cancer radiotherapy. Transl Androl Urol. 2018;7(3):445–458. [PubMed: 30050803]
44. Padgett KR, Swallen A, Pirozzi S, et al. Towards a universal MRI atlas of the prostate and prostate zones : Comparison of MRI vendor and image acquisition parameters. Strahlenther Onkol. 2018.
45. Zavala-Romero O, Breto AL, Xu IR, et al. Segmentation of prostate and prostate zones using deep learning : A multi-MRI vendor analysis. Strahlenther Onkol. 2020.
46. Mecke KR. Additivity, Convexity, and Beyond: Applications of Minkowski Functionals in Statistical Physics. 2000; Berlin, Heidelberg.
47. Johnson P, Young L, Lamichhane N, Patel V, Chinea F, Yang F. Quantitative imaging: correlating image features with the segmentation accuracy of PET based tumor contours in the lung. Radiother Oncol. 2017;123(2):257–262. [PubMed: 28433412]
48. Li BL. Fractal dimensions. Wiley Online Library; 2002.
49. Amadasun M, King R. Textural features corresponding to textural properties. IEEE Transactions on systems, man, and Cybernetics. 1989;19(5):1264–1274.
50. Haralick RM. Statistical and structural approaches to texture. Proceedings of the IEEE. 1979;67(5):786–804.
51. Loh H, Leu J, Luo RC. The analysis of natural textures using run length features. IEEE Transactions on Industrial Electronics. 1988;35(2):323–328.
52. Thibault G, Fertil B, Navarro C, et al. Texture indexes and gray level size zone matrix: application to cell nuclei classification. Paper presented at: Pattern Recognition and Information Processing 2009.
53. Bigun J. Speed, frequency, and orientation tuned 3-d gabor filter banks and their design. Paper presented at: Pattern Recognition, 1994. Vol. 3-Conference C: Signal Processing, Proceedings of the 12th IAPR International Conference on1994;
54. Ganeshan B, Miles KA, Young RC, Chatwin CR. Three-dimensional selective-scale texture analysis of computed tomography pulmonary angiograms. Investigative radiology. 2008;43(6):382–394. [PubMed: 18496043]
55. Mallat S A wavelet tour of signal processing. Academic press; 1999.
56. Varghese B, Chen F, Hwang D, et al. Objective risk stratification of prostate cancer using machine learning and radiomics applied to multiparametric magnetic resonance images. Scientific Reports. 2019;9(1):1570. [PubMed: 30733585]
57. Cuocolo R, Stanzione A, Ponsiglione A, et al. Clinically significant prostate cancer detection on MRI: A radiomic shape features study. European Journal of Radiology. 2019;116:144–149. [PubMed: 31153556]

58. Algohary A, Viswanath S, Shiradkar R, et al. Radiomic features on MRI enable risk categorization of prostate cancer patients on active surveillance: Preliminary findings. Journal of Magnetic Resonance Imaging. 2018;48(3):818–828.
59. Shiradkar R, Ghose S, Jambor I, et al. Radiomic features from pretreatment biparametric MRI predict prostate cancer biochemical recurrence: Preliminary findings. Journal of Magnetic Resonance Imaging. 2018;48(6):1626–1636. [PubMed: 29734484]
60. Bourbonne V, Fournier G, Vallières M, et al. External Validation of an MRI-Derived Radiomics Model to Predict Biochemical Recurrence after Surgery for High-Risk Prostate Cancer. Cancers. 2020;12(4).
61. van der Leest M, Israel B, Cornel EB, et al. High Diagnostic Performance of Short Magnetic Resonance Imaging Protocols for Prostate Cancer Detection in Biopsy-naive Men: The Next Step in Magnetic Resonance Imaging Accessibility. Eur Urol. 2019;76(5):574–581. [PubMed: 31167748]
62. Yang F, Ford JC, Dogan N, et al. Magnetic resonance imaging (MRI)-based radiomics for prostate cancer radiotherapy. Transl Androl Urol. 2018;7(3):445–458. [PubMed: 30050803]
63. Abdollahi H, Mofid B, Shiri I, et al. Machine learning-based radiomic models to predict intensity-modulated radiation therapy response, Gleason score and stage in prostate cancer. Radiol Med. 2019;124(6):555–567. [PubMed: 30607868]
64. Pollack A, Chinea FM, Bossart E, et al. Phase I Trial of MRI-Guided Prostate Cancer Lattice Extreme Ablative Dose (LEAD) Boost Radiation Therapy. International Journal of Radiation Oncology*Biology*Physics. 2020;107(2):305–315.
65. Chindasombatjaroen J, Kakimoto N, Murakami S, Maeda Y, Furukawa S. Quantitative analysis of metallic artifacts caused by dental metals: comparison of cone-beam and multi-detector row CT scanners. Oral Radiology. 2011;27(2):114–120.
66. Lechuga L, Weidlich GA. Cone Beam CT vs. Fan Beam CT: A Comparison of Image Quality and Dose Delivered Between Two Differing CT Imaging Modalities. Cureus. 2016;8(9):e778–e778. [PubMed: 27752404]
67. Nagarajappa AK, Dwivedi N, Tiwari R. Artifacts: The downturn of CBCT image. J Int Soc Prev Community Dent. 2015;5(6):440–445. [PubMed: 26759795]
68. Nardi C, Borri C, Regini F, et al. Metal and motion artifacts by cone beam computed tomography (CBCT) in dental and maxillofacial study. La radiologia medica. 2015;120(7):618–626. [PubMed: 25634792]
69. Bagher-Ebadian H, Siddiqui F, Liu C, Movsas B, Chetty IJ. On the impact of smoothing and noise on robustness of CT and CBCT radiomics features for patients with head and neck cancers. Medical Physics. 2017;44(5):1755–1770. [PubMed: 28261818]
70. Fave X, Mackin D, Yang J, et al. Can radiomics features be reproducibly measured from CBCT images for patients with non-small cell lung cancer? Medical Physics. 2015;42(12):6784–6797. [PubMed: 26632036]
71. Hall WA, Paulson ES, van der Heide UA, et al. The transformation of radiation oncology using real-time magnetic resonance guidance: A review. Eur J Cancer. 2019;122:42–52. [PubMed: 31614288]
72. Pathmanathan AU, van As NJ, Kerkmeijer LGW, et al. Magnetic Resonance Imaging-Guided Adaptive Radiation Therapy: A “Game Changer” for Prostate Treatment? Int J Radiat Oncol. 2018;100(2):361–373.
73. Boldrini L, Cusumano D, Chiloiro G, et al. Delta radiomics for rectal cancer response prediction with hybrid 0.35 T magnetic resonance-guided radiotherapy (MRgRT): a hypothesis-generating study for an innovative personalized medicine approach. La radiologia medica. 2018.
74. Simpson G, Spieler B, Dogan N, et al. Predictive value of 0.35 T magnetic resonance imaging radiomic features in stereotactic ablative body radiotherapy of pancreatic cancer: A pilot study. Med Phys. 2020.
75. Stoyanova R, Pollack A, Takhar M, et al. Association of multiparametric MRI quantitative imaging features with prostate cancer gene expression in MRI-targeted prostate biopsies. Oncotarget. 2016;7(33):53362–53376. [PubMed: 27438142]

76. Renard-Penna R, Cancel-Tassin G, Comperat E, et al. Multiparametric Magnetic Resonance Imaging Predicts Postoperative Pathology but Misses Aggressive Prostate Cancers as Assessed by Cell Cycle Progression Score. J Urol. 2015;194(6):1617–1623. [PubMed: 26272031]
77. Varlotto J, Stevenson MA. Anemia, tumor hypoxemia, and the cancer patient. Int J Radiat Oncol Biol Phys. 2005;63(1):25–36. [PubMed: 16111569]
78. Bristow RG, Hill RP. Hypoxia and metabolism. Hypoxia, DNA repair and genetic instability. Nat Rev Cancer. 2008;8(3):180–192. [PubMed: 18273037]
79. Vaupel P Tumor microenvironmental physiology and its implications for radiation oncology. Semin Radiat Oncol. 2004;14(3):198–206. [PubMed: 15254862]
80. Bache M, Kappler M, Said HM, Staab A, Vordermark D. Detection and specific targeting of hypoxic regions within solid tumors: current preclinical and clinical strategies. Curr Med Chem. 2008;15(4):322–338. [PubMed: 18288988]
81. Tatum JL, Kelloff GJ, Gillies RJ, et al. Hypoxia: importance in tumor biology, noninvasive measurement by imaging, and value of its measurement in the management of cancer therapy. Int J Radiat Biol. 2006;82(10):699–757. [PubMed: 17118889]
82. Cho H, Ackerstaff E, Carlin S, et al. Noninvasive multimodality imaging of the tumor microenvironment: registered dynamic magnetic resonance imaging and positron emission tomography studies of a preclinical tumor model of tumor hypoxia. Neoplasia. 2009;11(3):247–259, 242p following 259. [PubMed: 19242606]
83. Stoyanova R, Huang K, Sandler K, et al. Mapping Tumor Hypoxia In Vivo Using Pattern Recognition of Dynamic Contrast-enhanced MRI Data. Transl Oncol. 2012;5(6):437–447. [PubMed: 23326621]
84. Erho N, Crisan A, Vergara IA, et al. Discovery and validation of a prostate cancer genomic classifier that predicts early metastasis following radical prostatectomy. PLoS One. 2013;8(6):e66855. [PubMed: 23826159]
85. Den RB, Feng FY, Showalter TN, et al. Genomic prostate cancer classifier predicts biochemical failure and metastases in patients after postoperative radiation therapy. Int J Radiat Oncol Biol Phys. 2014;89(5):1038–1046. [PubMed: 25035207]
86. Den RB, Yousefi K, Trabulsi EJ, et al. Genomic classifier identifies men with adverse pathology after radical prostatectomy who benefit from adjuvant radiation therapy. Journal of clinical oncology : official journal of the American Society of Clinical Oncology. 2015;33(8):944–951. [PubMed: 25667284]
87. Klein EA, Yousefi K, Haddad Z, et al. A Genomic Classifier Improves Prediction of Metastatic Disease Within 5 Years After Surgery in Node-negative High-risk Prostate Cancer Patients Managed by Radical Prostatectomy Without Adjuvant Therapy. Eur Urol. 2015;67(4):778–786. [PubMed: 25466945]
88. Cuzick J, Berney DM, Fisher G, et al. Prognostic value of a cell cycle progression signature for prostate cancer death in a conservatively managed needle biopsy cohort. Br J Cancer. 2012;106(6):1095–1099. [PubMed: 22361632]
89. Freedland SJ, Gerber L, Reid J, et al. Prognostic utility of cell cycle progression score in men with prostate cancer after primary external beam radiation therapy. Int J Radiat Oncol Biol Phys. 2013;86(5):848–853. [PubMed: 23755923]
90. Cooperberg MR, Simko JP, Cowan JE, et al. Validation of a cell-cycle progression gene panel to improve risk stratification in a contemporary prostatectomy cohort. Journal of clinical oncology : official journal of the American Society of Clinical Oncology. 2013;31(11):1428–1434. [PubMed: 23460710]
91. Crawford ED, Scholz MC, Kar AJ, et al. Cell cycle progression score and treatment decisions in prostate cancer : results from an ongoing registry. Curr Med Res Opin. 2014;30(6):1025–1031. [PubMed: 24576172]
92. Badani KK, Thompson DJ, Brown G, et al. Effect of a genomic classifier test on clinical practice decisions for patients with high-risk prostate cancer after surgery. BJU international. 2015;115(3):419–429. [PubMed: 24784420]

93. Klein EA, Cooperberg MR, Magi-Galluzzi C, et al. A 17-gene assay to predict prostate cancer aggressiveness in the context of Gleason grade heterogeneity, tumor multifocality, and biopsy undersampling. Eur Urol. 2014;66(3):550–560. [PubMed: 24836057]
94. Knezevic D, Goddard AD, Natraj N, et al. Analytical validation of the Oncotype DX prostate cancer assay - a clinical RT-PCR assay optimized for prostate needle biopsies. BMC genomics. 2013;14:690. [PubMed: 24103217]
95. Cullen J, Rosner IL, Brand TC, et al. A Biopsy-based 17-gene Genomic Prostate Score Predicts Recurrence After Radical Prostatectomy and Adverse Surgical Pathology in a Racially Diverse Population of Men with Clinically Low- and Intermediate-risk Prostate Cancer. Eur Urol. 2015;68(1):123–131. [PubMed: 25465337]
96. Badani K, Kemeter M, Febbo PG, et al. The Impact of a Biopsy Based 17-Gene Genomic Prostate Score on Treatment Recommendations in Men with Newly Diagnosed Clinically Prostate Cancer Who are Candidates for Active Surveillance *Urology Practice*. 2015;2(4):181–189.
97. Hectors SJ, Cherny M, Yadav KK, et al. Radiomics Features Measured with Multiparametric Magnetic Resonance Imaging Predict Prostate Cancer Aggressiveness. J Urol. 2019;202(3):498–505. [PubMed: 30958743]
98. Zhao SG, Chang SL, Spratt DE, et al. Development and validation of a 24-gene predictor of response to postoperative radiotherapy in prostate cancer: a matched, retrospective analysis. Lancet Oncol. 2016;17(11):1612–1620. [PubMed: 27743920]
99. Woo S, Han S, Kim TH, et al. Prognostic Value of Pretreatment MRI in Patients With Prostate Cancer Treated With Radiation Therapy: A Systematic Review and Meta-Analysis. Am J Roentgenol. 2020;214(3):597–604. [PubMed: 31799874]
100. Wibmer A, Hricak H, Gondo T, et al. Haralick texture analysis of prostate MRI: utility for differentiating non-cancerous prostate from prostate cancer and differentiating prostate cancers with different Gleason scores. Eur Radiol. 2015;25(10):2840–2850. [PubMed: 25991476]
101. Vignati A, Mazzetti S, Giannini V, et al. Texture features on T2-weighted magnetic resonance imaging: new potential biomarkers for prostate cancer aggressiveness. Physics in Medicine and Biology. 2015;60(7):2685–2701. [PubMed: 25768265]
102. Fehr D, Veeraraghavan H, Wibmer A, et al. Automatic classification of prostate cancer Gleason scores from multiparametric magnetic resonance images. Proc Natl Acad Sci U S A. 2015;112(46):E6265–6273. [PubMed: 26578786]
103. Chaddad A, Kucharczyk MJ, Niazi T. Multimodal radiomic features for the predicting gleason score of prostate cancer. Cancers. 2018;10(8):249.
104. Chen T, Li M, Gu Y, et al. Prostate Cancer Differentiation and Aggressiveness: Assessment With a Radiomic-Based Model vs. PI-RADS v2. Journal of Magnetic Resonance Imaging. 2019;49(3):875–884. [PubMed: 30230108]
105. Min X, Li M, Dong D, et al. Multi-parametric MRI-based radiomics signature for discriminating between clinically significant and insignificant prostate cancer: Cross-validation of a machine learning method. European Journal of Radiology. 2019;115:16–21. [PubMed: 31084754]
106. Toivonen J, Montoya Perez I, Movahedi P, et al. Radiomics and machine learning of multisequence multiparametric prostate MRI: Towards improved non-invasive prostate cancer characterization. PloS one. 2019;14(7):e0217702 Accessed 2019. [PubMed: 31283771]
107. Abdollahi H, Mofid B, Shiri I, et al. Machine learning-based radiomic models to predict intensity-modulated radiation therapy response, Gleason score and stage in prostate cancer. La radiologia medica. 2019;124(6):555–567. [PubMed: 30607868]
108. Gong L, Xu M, Fang M, et al. Noninvasive Prediction of High-Grade Prostate Cancer via Biparametric MRI Radiomics. Journal of Magnetic Resonance Imaging. 2020;n/a(n/a).
109. Li M, Chen T, Zhao W, et al. Radiomics prediction model for the improved diagnosis of clinically significant prostate cancer on biparametric MRI. Quant Imaging Med Surg. 2020;10(2):368–379. [PubMed: 32190563]
110. Stoyanova R, Chinea F, Kwon D, et al. An Automated Multiparametric MRI Quantitative Imaging Prostate Habitat Risk Scoring System for Defining External Beam Radiation Therapy Boost Volumes. International Journal of Radiation Oncology*Biology*Physics. 2018;102(4):821–829.

111. Bleker J, Kwee TC, Dierckx RAJO, de Jong IJ, Huisman H, Yakar D Multiparametric MRI and auto-fixed volume of interest-based radiomics signature for clinically significant peripheral zone prostate cancer. European Radiology. 2020;30(3):1313–1324. [PubMed: 31776744]

112. Brunese L, Mercaldo F, Reginelli A, Santone A. Formal methods for prostate cancer Gleason score and treatment prediction using radiomic biomarkers. Magnetic Resonance Imaging. 2020;66:165–175. [PubMed: 31476359]

113. Tiwari P, Kurhanewicz J, Madabhushi A. Multi-kernel graph embedding for detection, Gleason grading of prostate cancer via MRI/MRS. Med Image Anal. 2013;17(2):219–235. [PubMed: 23294985]

114. Nketiah G, Elschot M, Kim E, et al. T2-weighted MRI-derived textural features reflect prostate cancer aggressiveness: preliminary results. Eur Radiol. 2017;27(7):3050–3059. [PubMed: 27975146]

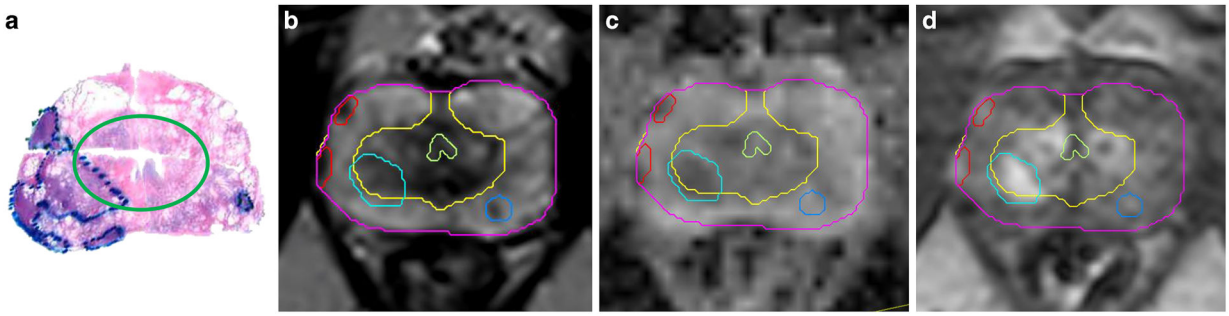

Figure 1. Correlation of radical prostatectomy histopathology with mpMRI.

a) Transverse pseudo whole mount section of H&E-stained radical prostatectomy from a patient with prostate cancer. The areas of the tumors are marked by pathologist. The green ellipse separates the peripheral (outer) and transition zones of the prostate; **b)** Corresponding T2-weighted axial MRI image is shown. The prostate is contoured in magenta. The two zones of the prostate have different intensities: the T2 signal is bright on the peripheral zone (yellow contour), due to the fact that the peripheral zone contains mainly prostatic acini and ducts and the prostatic fluid in their lumina rises a strong signal. Alternatively, the transition zone has a higher proportion of prostatic stroma. The light green structure is the urethra. Correspondingly, on the histopathology sample, the transition zone is surrounded by a porous tissue related to the frequent glandular luminae in the peripheral zone. The tumors (red and shades of blue) on T2-weighted MRI are hypo-intense. **c)** Apparent Diffusion Coefficient (ADC) image. ADC is calculated from Diffusion weighted imaging (DWI) - a specialized acquisition technique which highlights areas with restricted microscopic motion of water molecules. Tumors on ADC are also hypo-intense. **d)** The early enhancing image in the Dynamic Contrast Enhanced (DCE-) MRI. DCE-MRI highlights the tumor vasculature and areas of the tumor are of higher intensity.

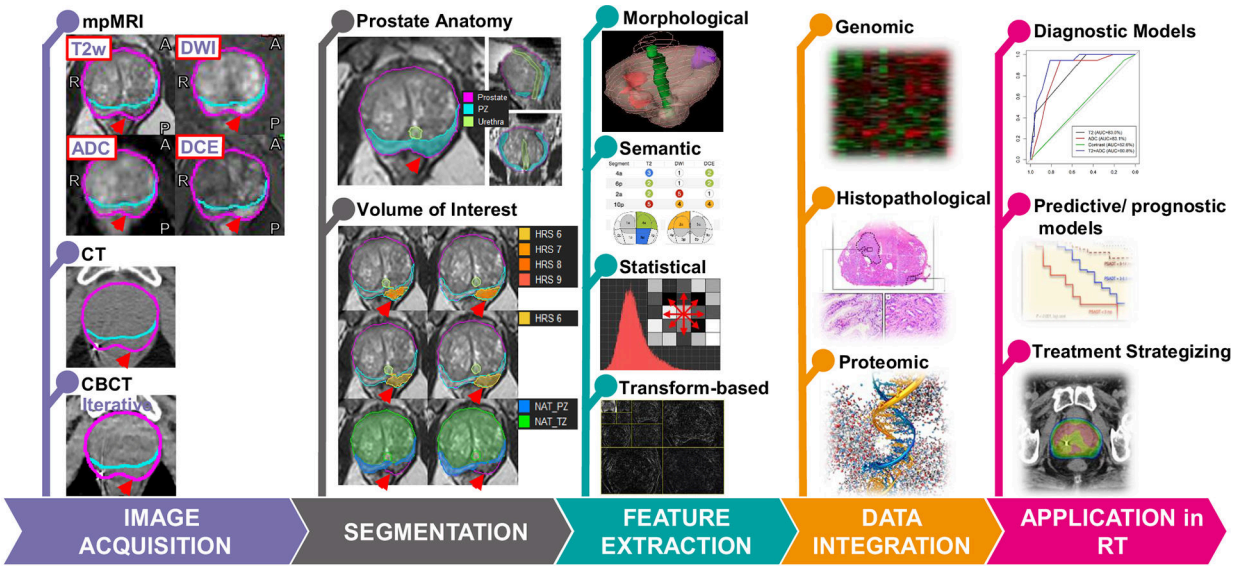

Figure 2. The radiomics workflow in RT of prostate cancer.

Image Acquisition: Image modalities, mpMRI, CT and CBCT from the same prostate cancer patient are shown. The red arrow points at the tumor. ***Segmentation:*** Prostate, urethra, peripheral zone (PZ), and transition zone (TZ), as shown in the top panel, are contoured. Habitat Risk Score (HRS), displayed as a heat map on the T2-weighted MRI indicates the tumor. HRS6 volume is selected for volume of interest (VOI) for radiomics features extraction (HRS6 also defines gross tumor volume (GTV)). Normal Appearing Tissues (NAT) in PZ and TZ are obtained by subtracting VOI from PZ and TZ. ***Feature extraction:*** The radiomics features typically belong to one of four categories shown. ***Data integration*****:** Radiomics features are integrated with other available biomarkers, such as data from clinical records, genomic profiling, proteomic screening, and physiological analysis. ***Application in RT:*** Integrated data/models are used to aid in diagnostic assessment, to facilitate patient-individualized treatment strategizing, and improve predictive and prognostic accuracy.

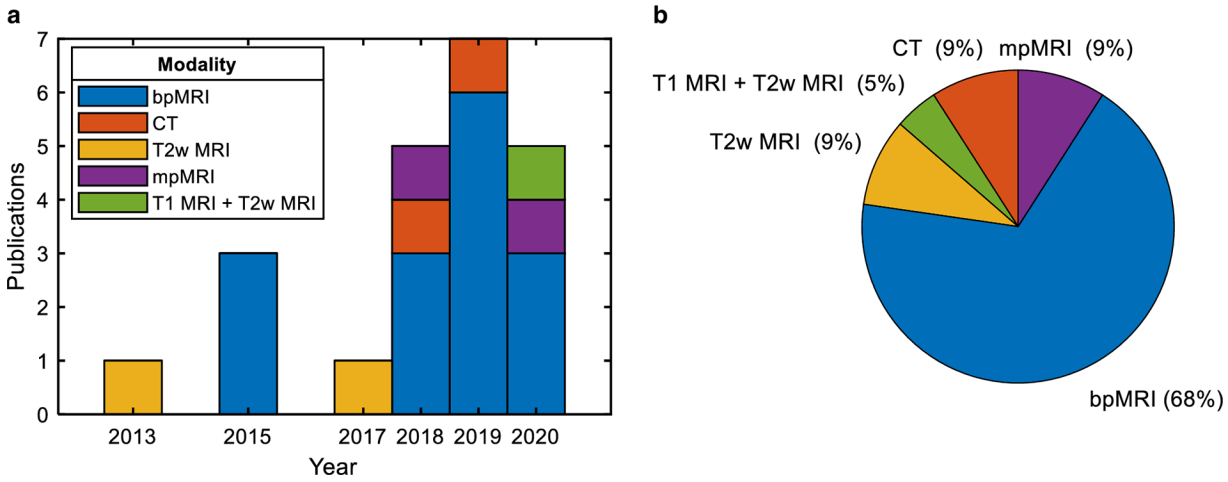

Figure 3:

Summary of publications to date that assessed tumor aggressiveness of prostate cancer using radiomics by **a)** the number of publications per year and **b)** the percentage of publications per modality.

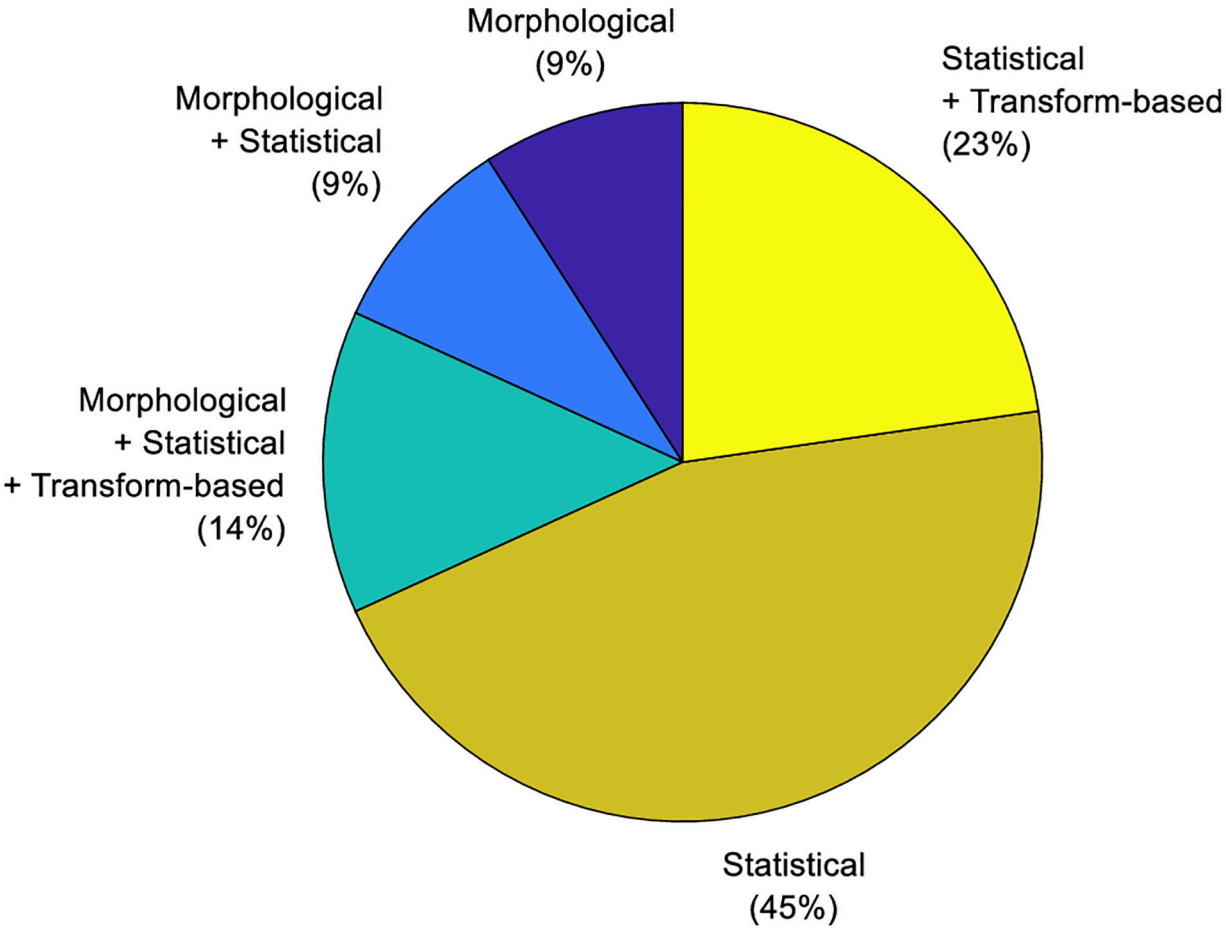

Figure 4:

A pie chart showing the proportion of publications to date according to the radiomic feature categories used to assess tumor aggressiveness of prostate cancer using radiomics.

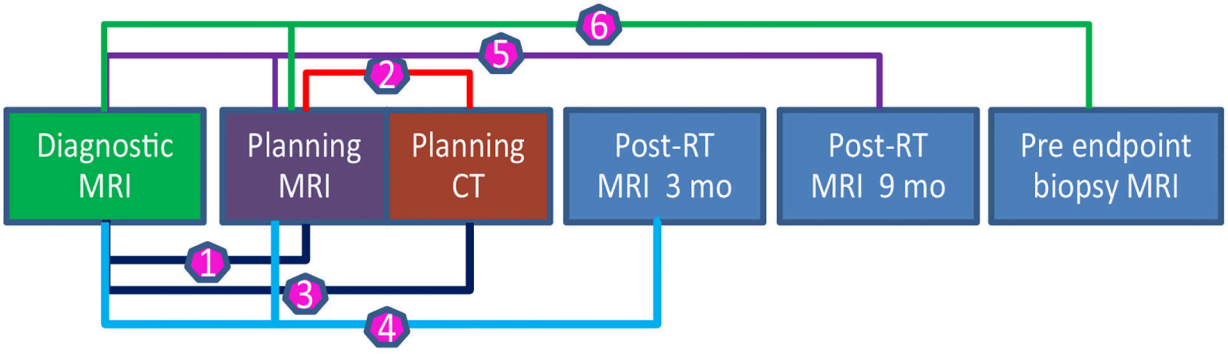

Figure 5. Adapted workflow for comparisons of pre- and post-treatment mpMRIs in prostate cancer radiotherapy clinical trials at the University of Miami.

Six image fusions are carried out, indicated on the graph above. (1) Using prostate anatomical matching, the diagnostic MRI is fused with the planning MRI; (2) The planning MRI is fused to the planning CT, using fiducial matching; (3) Using (1) and (2), the diagnostic MRI is fused to the planning MR for target volume contouring; (4–6) The post-RT MRIs (at 3 and 9 mo) and the one before the endpoint biopsy (2.0 – 2.5 yr after completion of all therapy) is fused with both the pre-RT planning and diagnostic MRI.

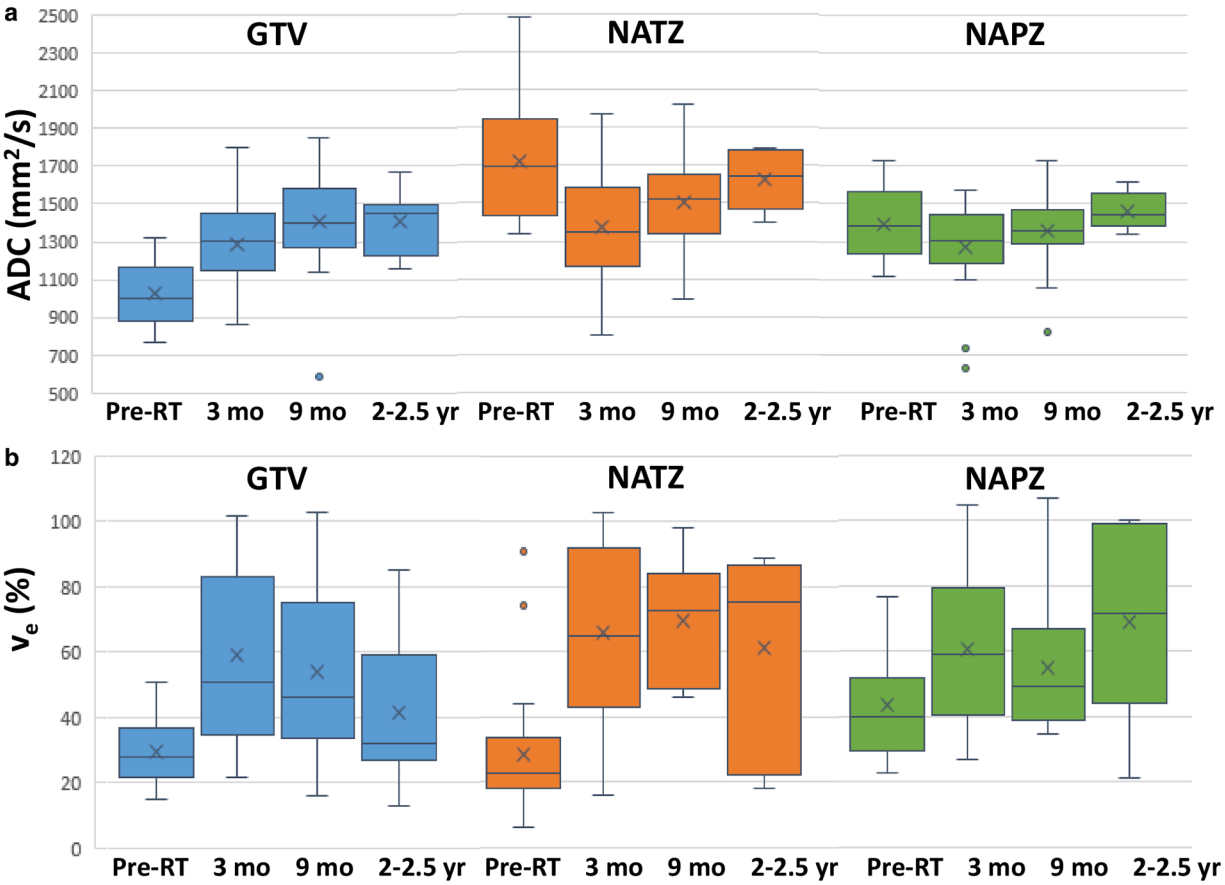

Figure 6. Delta radiomics in mpMRI (LEAD trial, University of Miami).

Using the workflow from Figure 5, radiomics features are extracted from gross tumor volume (GTV), normal appearing transition and peripheral zone (NATZ and NAPZ) at 3 mo and 9 mo after RT and 2–2.5 yr after end of all therapy. Box plots of Apparent diffusion coefficient (ADC) (upper series) and v_e (percent of extravascular extracellular space (EES)) (lower series).

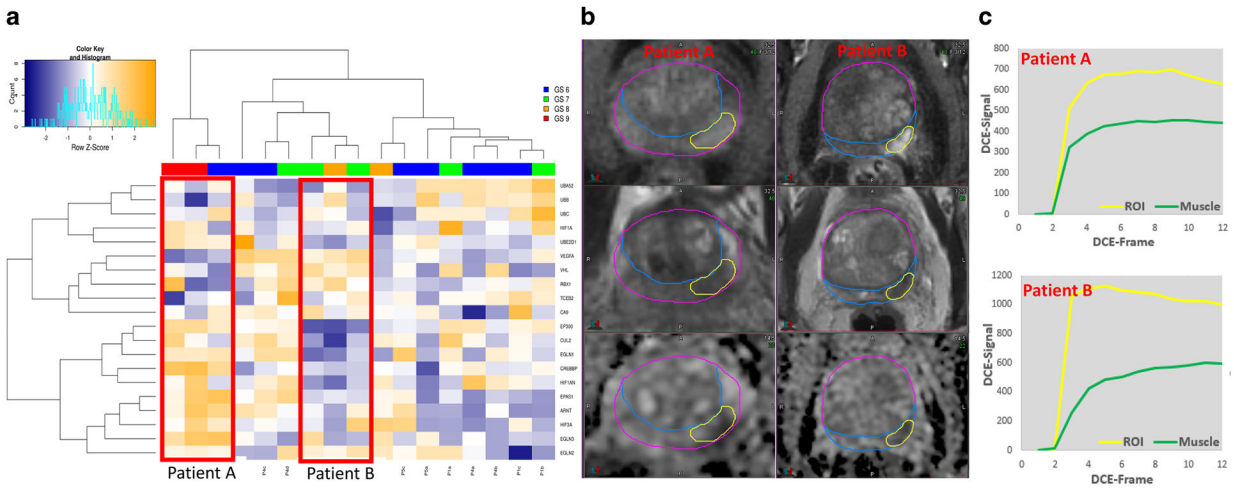

Figure 7. Association of Dynamic Contrast Enhanced (DCE-) MRI with hypoxia.

a) Hierarchical clustering on expression of the twenty hypoxia genes in 17 biopsies from 6 patients. Each sample is color-coded based on Gleason Score (GS). The two main clusters of genes were driven by the biopsy cores (n = 3) from two patients with high risk (marked with red boxes, Patient A and Patient B) Hypoxic genes, such as HIF3A, EPAS1, CUL2, EP300 are upregulated in the tissue from Patient A and vice versa, downregulated in the tissue from Patient B. **b)** Early enhancing series on DCE-MRI and corresponding T2-weighted and Apparent Diffusion Coefficient (ADC) images from Patient A and B. The enhancement is more pronounced in Patient B, suggesting well-perfused tumor. **c)** DCE-curves in the tumors, referenced to DCE signal in muscle (Gluteus Maximus). The tumor DCE-curves in Patient A are characterized with slower contrast uptake and moderate enhancement, characteristic for hypoxic tumors. On the other hand, in Patient B contrast uptake is hast and with high amplitude, suggesting well perfused tumor. Note that the muscle contrast-uptake amplitude is almost the same for the two patients.

Table 1:

Summary of radiomic manuscripts in prostate cancer, grouped by modality.

Reference	Tumor Segmentation	Modality	Feature Category	Analysis Endpoints	Performance
Wibmer *et al.* (2015)[100]	Manual	bpMRI	Statistical	Prostate cancer GS	p: <.0001 to .0008 p: .0019 to .0225
Vignati *et al.* (2015)[101]	Manual	bpMRI	Statistical	GS	AUC: 0.82 to 0.96
Fehr *et al.* (2015)[102]	Manual	bpMRI	Statistical	GS	Accuracy: 83% to 93% AUC: 0.91 to 0.99
Algohary *et al.* (2018)[58]	Manual	bpMRI	Statistical	PI-RADS and Biopsy positivity	p < 0.001
Shiradkar *et al.* (2018)[59]	Manual	bpMRI	Statistical, Transform-based	BCR	AUC: 0.73 to 0.84
Chaddad *et al.* (2018)[103]	Automatic	bpMRI	Statistical	GS	AUC: 0.65 to 0.82
Chen *et al.* (2019)[104]	Manual	bpMRI	Morphological, Statistical	Prostate Cancer GS	AUC: 0.98 to 0.999 AUC: 0.87 to 0.93
Cuocolo *et al.* (2019)[57]	Manual	bpMRI	Morphological	GS and max cancer core length	AUC: 0.78 p: 0.002
Min *et al.* (2019)[105]	Manual	bpMRI	Morphological, Statistical, Transform-based	GS	AUC: 0.73 to 0.87
Toivonen *et al.* (2019)[106]	Manual	bpMRI	Morphological, Statistical, Transform-based	GS	AUC: 0.71 to 0.84
Abdollahi *et al.* (2019)[107]	Manual	bpMRI	Statistical	GS	AUC: 0.61 to 0.74
Varghese et al. (2019)[56]	Manual	bpMRI	Statistical, Transform-based	Risk group using TG, GS, and PSA	AUC: 0.92
Gong *et al.* (2020)[108]	Manual	bpMRI	Morphological, Statistical	GS	AUC: 0.79 to 0.80
Li *et al.* (2020)[109]	Manual	bpMRI	Statistical	GS	AUC: 0.98
Bourbonne *et al.* (2020)[60]	Semi-automatic	bpMRI	Statistical, Transform-based	BCR	Accuracy: 76% to 78% AUC: 0.82 to 0.86
Stoyonova *et al.* (2018)[110]	Automatic	mpMRI	Statistical	GS	AUC: 0.72 to 0.90
Bleker *et al.* (2020)[111]	Auto-fixed	mpMRI	Statistical	GS	AUC: 0.87
Brunese *et al.* (2020)[112]	Manual	T1 MRI + T2w MRI	Morphological	GS	Sensitivity: 0.75 to 1 Specificity: 1
Tiwari *et al.* (2013)[113]	Automatic	T2w MRI	Statistical, Transform-based	GS	AUC: 0.84 to 0.89
Nketiah *et al.* (2017)[114]	Manual	T2w MRI	Statistical	GS	Accuracy: 91% AUC: 0.83
Tanadini-Lang *et al.* (2018)[12]	Manual	CT	Morphological, Statistical, Transform-based	GS	AUC: 0.77 to 0.81
Osman *et al.* (2019)[11]	Manual	CT	Statistical, Transform-based	GS Risk group using tumor grade, GS, and PSA	AUC: 0.90 to 1.00

Abbreviations: NAT = Normal Appearing Tissues; ROI = Region of Interest; GS = Gleason Score; BCR = Biochemical Recurrence; TG =Tumor Grade; AUC = Area under the Receiver Operating Characteristics curve (ROC).